Atmosphere drives recent interannual variability of the Atlantic meridional overturning circulation at 26.5°N

C. D. Roberts,[1] J. Waters,[2] K. A. Peterson,[1] M. D. Palmer,[1] G. D. McCarthy,[3]
E. Frajka-Williams,[4] K. Haines,[5] D. J. Lea,[2] M. J. Martin,[2] D. Storkey,[2]
E. W. Blockley,[2] and H. Zuo[6]

Received 8 July 2013; revised 30 August 2013; accepted 4 September 2013; published 1 October 2013.

[1] The Atlantic meridional overturning circulation (AMOC) has been observed at 26.5°N since 2004. During 2009/2010, there was a transient 30% weakening of the AMOC driven by anomalies in geostrophic and Ekman transports. Here, we use simulations based on the Met Office Forecast Ocean Assimilation Model (FOAM) to diagnose the relative importance of atmospheric forcings and internal ocean dynamics in driving the anomalous geostrophic circulation of 2009/2010. Data-assimilating experiments with FOAM accurately reproduce the mean strength and depth of the AMOC at 26.5°N. In addition, agreement between simulated and observed stream functions in the deep ocean is improved when we calculate the AMOC using a method that approximates the observing array at 26.5°N. The main features of the geostrophic circulation anomaly are captured by an ensemble of simulations without data assimilation. These model results suggest that the atmosphere played a dominant role in driving recent interannual variability of the AMOC. **Citation:** Roberts, C. D., et al. (2013), Atmosphere drives recent interannual variability of the Atlantic meridional overturning circulation at 26.5°N, *Geophys. Res. Lett.*, *40*, 5164–5170, doi:10.1002/grl.50930.

1. Introduction

[2] The AMOC is responsible for ∼90% of the northward ocean heat transport in the subtropical North Atlantic [*Johns et al.*, 2011] and is believed to have a significant influence on the mean state [*Vellinga and Wood*, 2002] and variability [*Latif and Keenlyside*, 2011] of North Atlantic climate. In addition, evidence for abrupt changes in paleoclimate records have been linked to changes in the state of the AMOC [*McManus et al.*, 2004] and modeling studies have shown that the AMOC is an important source of potential predictability [*Collins et al.*, 2006].

[3] Since April 2004, the RAPID meridional overturning circulation and heatflux array (hereafter referred to as "RAPID") array has made continuous observations of the strength and vertical structure of the AMOC at 26.5°N [*Cunningham et al.*, 2007], allowing investigation of AMOC variability on previously unresolved timescales. From 1 April 2004 to 31 March 2009, the AMOC at 26.5°N had a strength of 18.5 ± 1.0 Sv (mean ± standard deviation of annual means). However, this period of stability was followed by a decrease of the AMOC during 2009/2010, when the annual mean AMOC was reduced by 5.7 Sv compared to the 2004–2008 mean [*McCarthy et al.*, 2012]. This variability was driven by a 2.9 Sv increase in the southward upper-mid ocean (UMO) circulation, a 1.7 Sv decrease of Ekman transports associated with an extremely negative phase of the North Atlantic Oscillation, and a 1.1 Sv decrease of the Florida Current (FC). Changes to the geostrophic transport in the mid-ocean were associated with a deepening of the thermocline at the western boundary. Until now, the relative importance of atmosphere forcings and internal ocean dynamics in driving this anomaly had not been diagnosed. The climatic impacts of this event are currently being investigated.

[4] AMOC observations provide a powerful constraint for the evaluation of meridional transports in model simulations. For example, recent studies have used RAPID data to evaluate mean transports at 26.5°N in ocean reanalyses [*Haines et al.*, 2012, 2013] and the seasonal cycle of the AMOC in a high-resolution ocean model [*Mielke et al.*, 2013]. Here, we focus on evaluating the variability of the AMOC and its components at 26.5°N in simulations based on the latest operational version of the UK Met Office Forecast Ocean Assimilation Model (FOAM) [*Waters et al.*, 2013], with a particular focus on the interannual variability observed during 2009/2010. In addition, we present results from an ensemble of simulations without data assimilation and use these results to quantify the fraction of AMOC variability that can be explained by the forcing from atmospheric boundary conditions.

2. Methods

[5] The latest version of FOAM (FOAM-3DVAR) is based on v3.2 of the Nucleus for European Modelling of the Ocean (NEMO) global ocean model [*Madec*, 2008] configured with 75 vertical z levels and a nominal horizontal resolution of ∼0.25° coupled to the CICE v4.1 sea ice model [*Hunke and Lipscomb*, 2010]. In the experiments presented here, surface boundary conditions are specified as 3-hourly fields of 10 m winds, 2 m air temperature, 2 m

Additional supporting information may be found in the online version of this article.

[1]Met Office Hadley Centre, Exeter, UK.
[2]Met Office, Exeter, UK.
[3]National Oceanography Centre, Southampton, UK.
[4]Department of Ocean and Earth Science, University of Southampton, Southampton, UK.
[5]Department of Meteorology, University of Reading, Reading, UK.
[6]European Centre for Medium-Range Weather Forecasts, Reading, UK.

Corresponding author: C. D. Roberts, Met Office Hadley Centre, Fitzroy Rd., Exeter, EX1 3PB, UK. (chris.roberts@metoffice.gov.uk)

0094-8276/13/10.1002/grl.50930

This article was corrected on 27 May 2014. See the end of the full text for details.

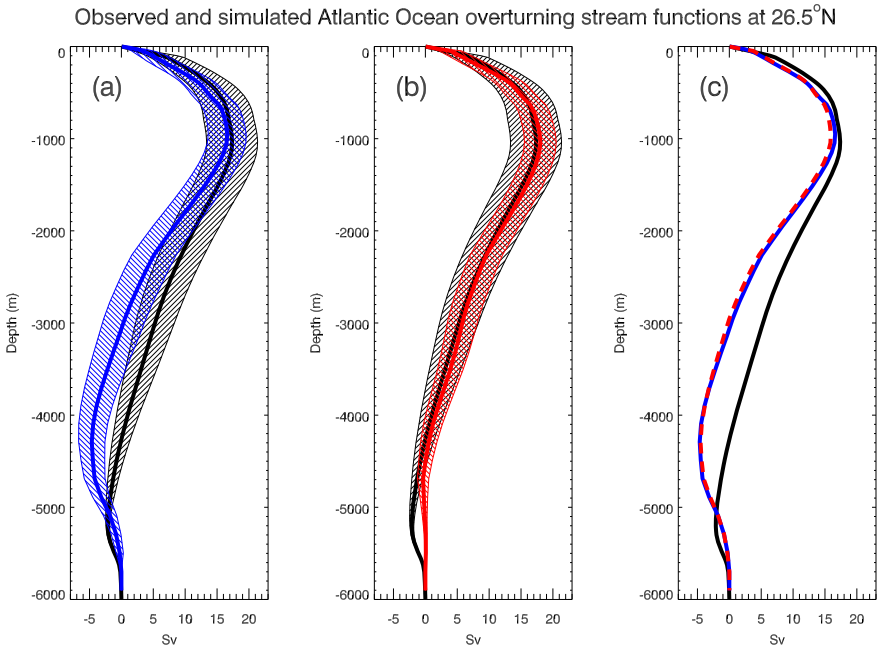

Figure 1. Time mean Atlantic meridional overturning stream functions at 26.5°N from RAPID (black in Figures 1a, 1b, and 1c) compared with overturning in ASSIM-3DVAR calculated using different methods: (a) Stream functions calculated using model velocities (blue). (b) Stream functions calculated using the RAPID-style method and a geostrophic reference depth of 4740 m (red). (c) Stream functions calculated using the RAPID-style method referenced to model velocities at 1000 m (dashed red line) compared with the mean profile (blue line) redrawn from Figure 1a. All calculations are for the period of January 2004 to December 2010, and hatching indicates a range of ±1 standard deviation calculated from monthly mean values.

specific humidity, short/long wave radiation, precipitation, and snowfall from the ERA-interim atmosphere reanalysis [*Dee et al.*, 2011]. Turbulent air-sea surface fluxes are calculated using the bulk formulae of *Large and Yeager* [2004], and data assimilation is performed using an incremental 3D-VAR scheme [*Waters et al.*, 2013]. Previous versions of FOAM are described by *Martin et al.* [2007] and *Storkey et al.* [2010] and further description of the FOAM-3DVAR system, including details of the data assimilation, is available as supporting information. Importantly, none of the experiments considered in this study assimilate in situ data from the RAPID array, so these data can be used as independent constraints to evaluate meridional transports.

[6] We describe results for the period 1 Jan 2004 to 31 Dec 2010 from the following simulations: (1) ASSIM-3DVAR is a data-assimilating ocean reanalysis based on FOAM-3DVAR. This experiment was initialized from rest in 1995 using the EN3 v2a gridded analysis of quality-controlled temperature and salinity data [*Ingleby and Huddleston*, 2007]. (2) NO-ASSIM is an 8-member initial condition ensemble from the FOAM-3DVAR system in which data assimilation and all restoring terms are disabled. Each experiment is 7 years long and initialized using a different ocean state from ASSIM-3DVAR (1 Jan of years 2004 to 2011). This ensemble allows us to estimate the relative contributions of atmospheric forcings and internal ocean dynamics in driving AMOC variability and is similar in design to the experiments described by *Hirschi et al.* [2012]. By averaging over the initial condition ensemble, variability due to "chaotic" behavior arising from the different initial conditions will be suppressed and the variability due to common atmospheric forcings will remain. (3) ASSIM-AC is a data-assimilating ocean reanalysis based on a previous version of FOAM [*Storkey et al.*, 2010]. This experiment has the same physical ocean model as ASSIM-3DVAR but uses a different sea ice model and an analysis correction data assimilation scheme [*Martin et al.*, 2007], which includes differences in the specification of error covariances multivariate balance relationships. The ASSIM-AC simulation was performed as part of the MyOcean project (http://www.myocean.eu/) and is described fully in *Haines et al.* [2013] (their experiment "UR025.4"). This data set is published and permanently available at the British Atmospheric Data Centre [*Zuo et al.*, 2013]. We have included analysis of this experiment in order to document the sensitivity of the AMOC to changes in the FOAM system.

3. Results

3.1. Calculation of the AMOC

[7] To observe the AMOC at 26.5°N, the RAPID array combines measurements of the Gulf Stream through the Florida Straits, Ekman transports calculated from zonal wind stress, western boundary transports measured using current meters, geostrophic transports measured with dynamic height moorings in the ocean interior, and a mass compensation term to ensure that there is zero net transport through the section [*Rayner et al.*, 2011]. In order to make the most appropriate comparisons, all model transports are calculated using an analogous "RAPID-style" methodology (see supporting information).

[8] To evaluate the vertical structure of the AMOC in ASSIM-3DVAR and to check our implementation of the

Table 1. Simulated and Observed Atlantic Ocean Meridional Transport Diagnostics at 26.5°N Calculated Using Monthly Means for the Period 01 April 2004 to 31 December 2010[a]

Experiment	Mean	Standard Deviation	Bias	Correlation (r^2)	Total Root-Mean-Square Error
AMOC at 26.5°N (Sv)					
RAPID	17.52	3.99	-	-	-
ASSIM-AC	17.82	4.56	0.30	0.53 (0.29)	4.14
ASSIM-3DVAR	17.69	2.85	0.18	0.75* (0.56)	2.65
NO-ASSIM	13.34	2.67	–4.17	0.78* (0.60)	4.88
Gulf Stream transport (Sv)					
RAPID	31.53	2.39	-	-	-
ASSIM-AC	29.25	3.00	–2.28	0.38 (0.14)	3.79
ASSIM-3DVAR	25.57	1.62	–5.97	0.54* (0.29)	6.30
NO-ASSIM	27.84	1.51	–3.69	0.41 (0.17)	4.31
Upper mid-ocean transport (Sv)					
RAPID	–17.15	2.94	-	-	-
ASSIM-AC	–13.98	3.38	3.16	0.52 (0.27)	4.43
ASSIM-3DVAR	–10.65	2.38	6.50	0.61 (0.37)	6.92
NO-ASSIM	–17.23	1.98	–0.09	0.71* (0.50)	2.08
Ekman transport (Sv)					
RAPID	3.19	2.29	-	-	-
ASSIM-AC	2.55	2.13	–0.64	0.99 (0.98)	0.75
ASSIM-3DVAR	2.77	2.13	–0.41	0.99 (0.98)	0.56
NO-ASSIM	2.74	2.10	–0.45	0.99 (0.98)	0.59

[a]Model diagnostics are calculated using the RAPID-style methodology for ASSIM-AC, ASSIM-3DVAR, and the NO-ASSIM ensemble mean. Stars indicate correlations that are significantly higher than the corresponding correlation in ASSIM-AC (see supporting information for statistical methods).

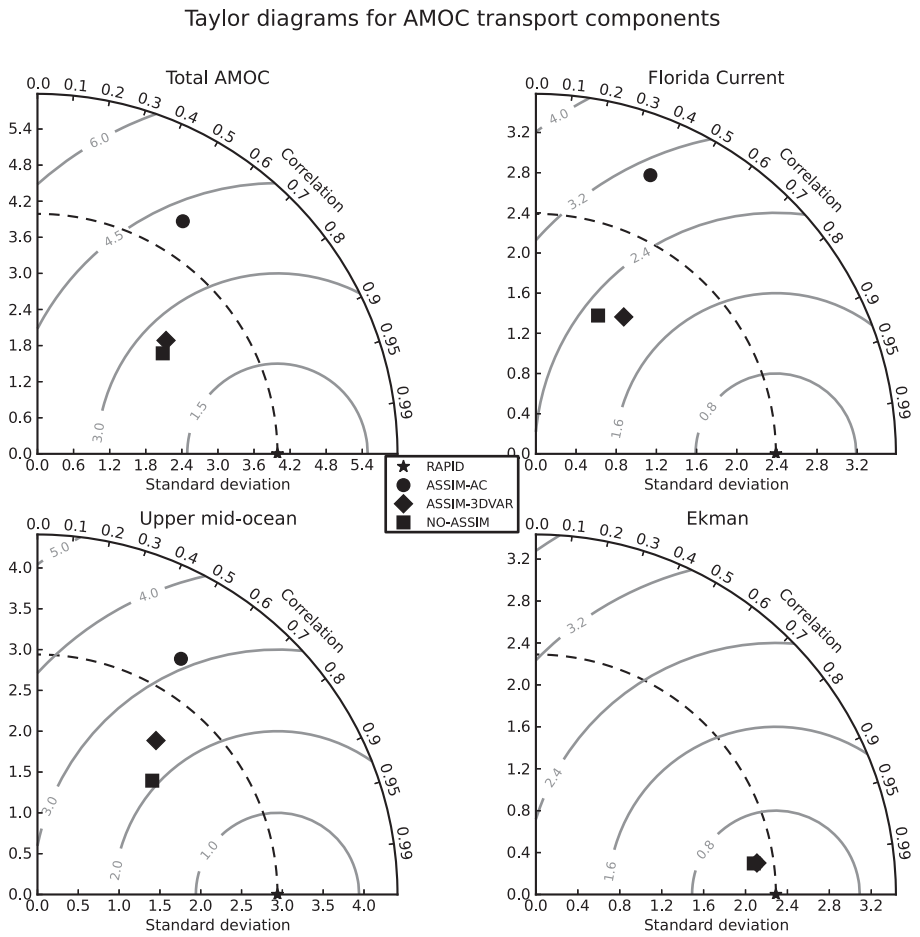

Figure 2. Taylor diagram showing correlations, standard deviations, and centered root-mean-square errors (gray contours) for each AMOC transport component at 26.5°N in ASSIM-3DVAR, ASSIM-AC, and the ensemble mean of NO-ASSIM.

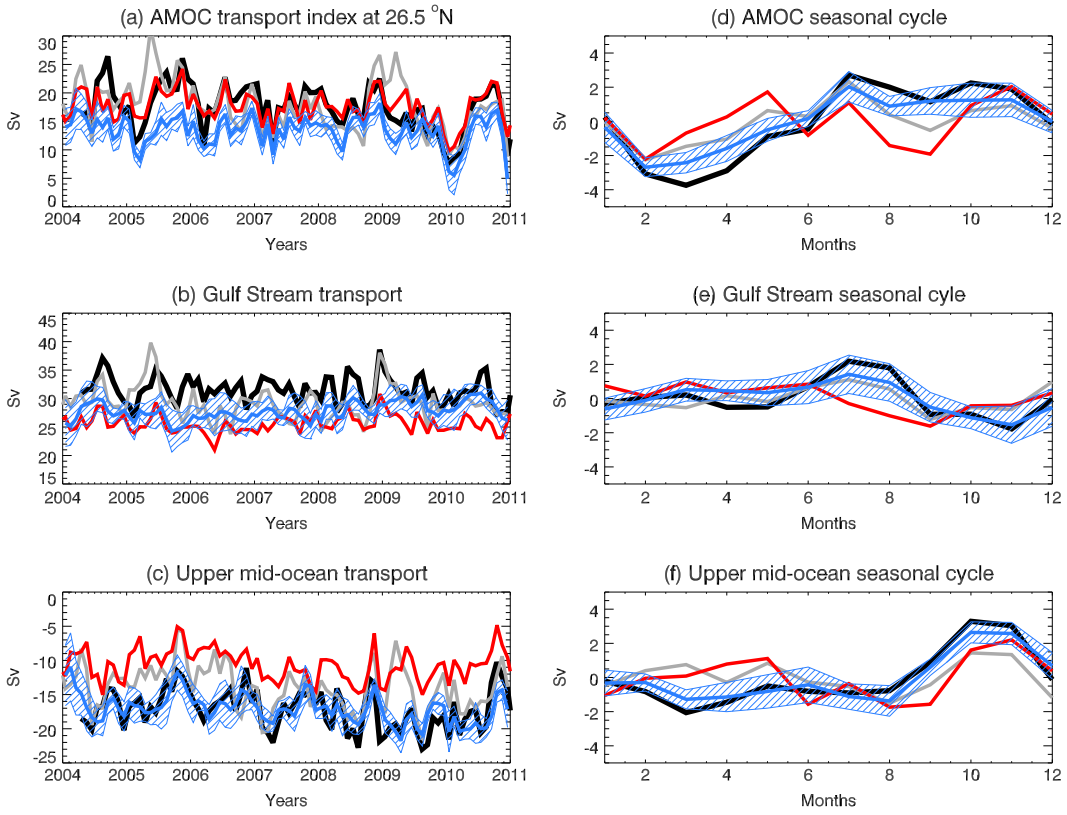

Figure 3. (a–c) Monthly mean time series of observed and simulated components of the AMOC from the RAPID array (black lines), ASSIM-3DVAR (red lines), ASSIM-AC (gray lines), and NO-ASSIM (blue lines with hatching covering mean ±2 standard deviations of the ensemble members). Transports are defined as the value of overturning stream functions at a depth of 1050 m for (a) total AMOC at 26.5°N, (b) Florida Current transports, and (c) upper-mid ocean transports. (d–f) Corresponding seasonal cycles for each AMOC component.

RAPID-style calculation, we compare stream functions from the RAPID array with simulated stream functions calculated from model data (Figure 1). We find that agreement between the simulated and observed AMOC is substantially improved when we calculate the AMOC using the observational methodology, particularly in the deep ocean. The differences between the two model profiles are due to a sensitivity to the choice of geostrophic reference level. When geostrophic velocities are referenced to model velocities at 1000 m, the true model overturning is recovered (Figure 1c). One of the reasons for the sensitivity to reference depth in the model calculations is that dynamic heights are referenced to the ocean bottom when the reference level intersects with topography. This zonally varying reference level causes a reduction in vertical shear of the calculated deep ocean transports (Figure S1 in the supporting information). It is not clear how this sensitivity should impact the transports calculated from the RAPID array because of the way shallow moorings are combined with deeper moorings to create merged boundary profiles. This sensitivity will be investigated in future work.

[9] The choice of reference level can also affect the deep structure of the overturning by requiring a change in the velocity applied as a mass conservation constraint. The magnitude of this sensitivity depends on the vertical shear of zonally integrated transport at depth. To evaluate the sensitivity of the RAPID calculations to the choice of reference level, we recalculate RAPID overturning profiles for a range of geostrophic reference levels (see Auxiliary methods and Figures S2 and S3 in the supporting information). These calculations reveal that the shape of the overturning at depth is sensitive to the the choice of reference level. For example, profiles calculated using a value of 1780 m are closer in structure to the profiles calculated from model velocities, although this solution has 3.5 Sv of Antarctic bottom water when observations indicate it should be about ∼ 2 Sv [*Hall et al.*, 1997]. All calculations agree on the maximum strength of the AMOC to within 2 Sv.

[10] These results highlight a potential uncertainty in the structure of the AMOC at depth, which could help explain some of the previously documented bias in the depth of the AMOC return flow in models [e.g., *Roberts et al.*, 2013; *Danabasoglu et al.*, 2010]. However, the reference level of 4740 m applied to the RAPID data was not determined arbitrarily. This value was chosen as it is the depth where zonally integrated transports from hydrographic sections are near zero, and it also results in a conservative application of the mass conservation constraint. Nevertheless, we note that a single reference level chosen to minimize the adjustment for mass conservation is not necessarily the best way to apply this constraint. A more sophisticated solution could use a zonally variable reference level that reflects differences in the depth of no motion across the section [e.g., *Atkinson et al.*, 2012]. Despite the sensitivities outlined above, all comparisons in the remainder of this paper are made using the RAPID-style methodology and a reference depth of 4740 m.

Table 2. Annual Means of Simulated and Observed Upper-mid Ocean Transports at 26.5°N in Sv[a]

	2004/05	2005/06	2006/07	2007/08	2008/09	2009/10	2004–2008 average	2009/10 minus 2004–2008 average
RAPID	–17.0	–15.5	–16.1	–17.1	–18.3	–19.7	–16.8	–2.9
NO-ASSIM ensemble mean	–17.0	–15.6	–16.8	–16.8	–17.8	–18.8	–16.8	–2.0
ASSIM-AC	–13.5	–11.1	–14.2	–14.5	–14.8	–15.2	–13.6	–1.6
ASSIM-3DVAR	–10.6	–8.8	–9.8	–11.8	–12.3	–11.5	–10.6	–0.8

[a]All annual means are calculated using the period 1 April to 31 March.

3.2. AMOC Mean State

[11] Summary statistics describing the mean state of each component of the AMOC are presented in Table 1. The total strength of the AMOC is simulated accurately in ASSIM-3DVAR (and ASSIM-AC) but is $\sim$ 4 Sv too low in the NO-ASSIM ensemble, thus indicating that data assimilation is providing a strong constraint on the total northward transport at 26.5°N. However, although ASSIM-3DVAR accurately simulates the net AMOC, there are compensating biases in FC and UMO transports. Similar biases are present in ASSIM-AC, although they are reduced in magnitude. UMO transports in NO-ASSIM are very close to the values observed by RAPID, although FC transports are too weak. All model experiments have near-identical Ekman transports as they share a common atmospheric forcing, and the small difference compared to the observations is due to the use of cross-calibrated multiplatform winds [*Atlas et al.*, 2011] in the RAPID data. For this reason, we will not consider Ekman transports any further in this study.

[12] To diagnose the cause of differences in UMO transports, we examine biases in profiles of mean density and dynamic height at the eastern and western boundaries (Figure S4). In the depth range 300–1000 m, all models show a positive density bias at the western boundary. However, in the depth range 0–300 m, density biases are negative and larger in magnitude in ASSIM-AC and NO-ASSIM compared to the positive biases in ASSIM-3DVAR. This change of sign to the density biases at the western boundary causes a reduction of near-surface dynamic height biases in ASSIM-AC and NO-ASSIM, leading to reduced biases in dynamic height gradient across the basin and better simulation of integrated transports in the ocean interior. The improvement to near-surface densities in ASSIM-3DVAR results in a deterioration of integrated meridional transports because only part of the compensating error field has been improved.

3.3. AMOC Variability

[13] Correlations and centered root-mean-square errors for monthly transports are improved in ASSIM-3DVAR and NO-ASSIM (compared to ASSIM-AC), but the magnitude of monthly variability is generally too weak compared to observations (Table 1, Figure 2). In addition, seasonal cycles in UMO and FC transports are too weak in ASSIM-3DVAR and ASSIM-AC, and the phase of the FC seasonal cycle is inaccurate in ASSIM-3DVAR (Figure 3). In contrast, seasonal cycles are well simulated by the ensemble mean of NO-ASSIM, indicating that prescription of atmospheric boundary conditions is the most important factor in driving seasonality of AMOC transports at 26.5°N. This comparison is consistent with previous studies, which have shown that seasonal cycles in FC, UMO and Ekman transports can be related to seasonal variability of local and remote wind forcings [*Kanzow et al.*, 2010; *Atkinson et al.*, 2010]. The cause of the impaired seasonal variability in ASSIM-3DVAR and ASSIM-AC compared to NO-ASSIM is currently unknown, but it is likely a consequence of the implemented data assimilation.

[14] All three experiments simulate a decrease of the AMOC during 2009/2010, although the magnitude of the total AMOC change is lower than observed. *McCarthy et al.* [2012] showed that the AMOC minimum during 2009/2010 was due to a combination of anomalies in Ekman, FC, and UMO transports, with the largest contribution coming from an increase in southward geostrophic transport in the ocean interior. Because the contribution from FC transports is relatively small, and given that Ekman transports are calculated from the prescribed wind field, we will focus our comparison on the simulation of the UMO transport anomaly.

[15] The ensemble mean of NO-ASSIM captures the majority of the observed variability of the UMO transports (Figure 3c and Table 2). Assuming a linear model, NO-ASSIM explains 50% of the observed monthly variance and 66% of the observed interannual variance (calculated using monthly values following the application of an 18 month low-pass filter). In contrast, ASSIM-3DVAR (ASSIM-AC) captures a smaller fraction of the observed UMO anomaly during 2009/2010 (Table 2) and explains only 37% (27%) of the monthly UMO transport variance. These results indicate that, in some cases, the assimilation of observations can cause an impairment in the simulation of atmosphere-forced transport variability on seasonal-to-interannual timescales.

[16] Based on the evidence above, we conclude that the majority of the interannual AMOC variability described by *McCarthy et al.* [2012] can be explained by variability in atmospheric boundary conditions. NO-ASSIM does not explain the small decrease in the FC during 2009/2010 (in fact it simulates a small increase during this period) suggesting that processes other than variability to atmospheric boundary conditions are important in driving this anomaly. This result is consistent with a recent study that described an influence of westward propagating eddies on the FC during 2009–2011 [*Frajka-Williams et al.*, 2013], which we would not expect to capture in an initial condition ensemble of simulations forced with atmospheric boundary conditions.

4. Discussion

[17] *Thomas and Zhai* [2013] suggested that the observed AMOC anomaly during 2009/2010 may have been a random event that was not linked to atmospheric boundary forcings. However, this inference was based on the presence of a similar magnitude AMOC anomaly in a 1/10° regional ocean model in which atmospheric forcings were prescribed as climatological monthly means, not on results from simulations with a time-evolving atmospheric forcing. In contrast,

Hirschi et al. [2012] found that 70–80% of AMOC variability in an eddy-permitting version of the NEMO model could be reconstructed from surface forcings. Our results are consistent with those of *Hirschi et al.* [2012], and we have been able to show that the observed AMOC anomaly in 2009/2010 is largely driven by the response of the UMO transports and Ekman layer to variability in atmospheric boundary conditions. For this reason, accurate prediction of the AMOC anomaly observed during 2009/2010 (and any resulting climate impacts) would require a forecast model capable of accurately predicting the observed anomalies in atmospheric boundary conditions. This conclusion is not necessarily in contradiction with the current seasonal-to-decadal climate prediction paradigm of predictability arising from ocean initial conditions. In particular, *Fereday et al.* [2012] found that predictability of the 2009/2010 North Atlantic Oscillation was linked to ocean initial conditions in the tropical Pacific, which ultimately affected atmospheric circulation in the North Atlantic through a stratospheric teleconnection.

[18] Given the importance of the AMOC as a source of potential predictability in the climate system, our results also have implications for the initialization of climate forecast models. Several recent studies have proposed a simple alternative to data assimilation whereby initial conditions are derived from a non-assimilating ocean model forced with observation-based atmospheric forcings [*Matei et al.*, 2012a, 2012b; *Yeager et al.*, 2012]. Our results confirm that it is possible to simulate the main features of AMOC variability at 26.5°N without data assimilation, albeit with an overturning circulation that is too weak. In contrast, we find that data assimilation provides a strong constraint on the absolute strength of the AMOC, but the seasonal cycle and interannual variability of geostrophic transports are impaired compared to the NO-ASSIM experiment. Determining the impact on forecast skill of the NO-ASSIM versus ASSIM-3DVAR initial conditions would require a dedicated set of hindcast experiments, which we have not performed. However, for there to be a significant improvement using NO-ASSIM, the small differences in the AMOC (and possibly other aspects of the ocean dynamics) would have to outweigh the many improvements to the ocean mean state imposed by the data assimilation.

5. Conclusions

[19] Using results from an updated version of the Met Office Forecast Ocean Assimilation model (FOAM-3DVAR), we have shown that data assimilation provides a strong constraint on the total AMOC at 26.5°N. We have also shown that agreement between the simulated and observed AMOC in the deep ocean is substantially improved when transports are calculated using the assumptions applied in the RAPID observations. Based on this comparison, we identify a sensitivity in the observed vertical structure of the AMOC to the choice of geostrophic reference depth, which could help explain some of the previously documented bias in the depth of the AMOC return flow in models. Month-to-month AMOC variability in FOAM-3DVAR is generally too weak. However, the main features of the observed geostrophic circulation anomaly during 2009/2010 are captured in an ensemble of simulations without data assimilation. From these results, we infer that atmospheric boundary conditions played a dominant role in driving the 2009/2010 anomaly in the AMOC.

[20] **Acknowledgments.** Data from the RAPID-MOCHA program are funded by the U.S. National Science Foundation and UK Natural Environment Research Council and are freely available at www.noc.soton.ac.uk/rapidmoc and www.rsmas.miami.edu/users/mocha. This work was supported by the Natural Environment Research Council and the Joint DECC/Defra Met Office Hadley Centre Climate Programme (GA01101). We thank Meric Srokosz and two anonymous reviewers for their useful comments on an earlier version of this manuscript.

[21] The Editor thanks two anonymous reviewers for their assistance in evaluating this paper.

References

Atkinson, C. P., H. L. Bryden, J. J.-M. Hirschi, and T. Kanzow (2010), On the seasonal cycles and variability of Florida Straits, Ekman and Sverdrup transports at 26°N in the Atlantic Ocean, *Ocean Sci.*, *6*(4), 837–859.

Atkinson, C. P., H. L. Bryden, S. A. Cunningham, and B. A. King (2012), Atlantic transport variability at 25°N in six hydrographic sections, *Ocean Sci. Discuss.*, *9*, 105–162.

Atlas, R., R. N. Hoffman, J. Ardizzone, S. M. Leidner, J. C. Jusem, D. K. Smith, and D. Gombos (2011), A cross-calibrated, multiplatform ocean surface wind velocity product for meteorological and oceanographic applications, *Bull. Am. Meteorol. Soc.*, *92*(2), 157–174.

Collins, M., et al. (2006), Interannual to decadal climate predictability in the North Atlantic: A multimodel-ensemble study, *J. Clim.*, *19*(7), 1195–1203.

Cunningham, S., et al. (2007), Temporal variability of the Atlantic meridional overturning circulation at 26.5°N, *Science*, *317*(5840), 935–938.

Danabasoglu, G., W. Large, and B. Briegleb (2010), Climate impacts of parameterized Nordic Sea overflows, *J. Geophys. Res.*, *115*, C11005, doi:10.1029/2010JC006243.

Dee, D., et al. (2011), The ERA-Interim reanalysis: Configuration and performance of the data assimilation system, *Q. J. R. Meteorolog. Soc.*, *137*(656), 553–597.

Fereday, D., A. Maidens, A. Arribas, A. Scaife, and J. Knight (2012), Seasonal forecasts of Northern Hemisphere winter 2009/10, *Environ. Res. Lett.*, *7*(3), 034031, doi:10.1088/1748-9326/7/3/034031.

Frajka-Williams, E., W. Johns, C. Meinen, L. Beal, and S. Cunningham (2013), Eddy impacts on the Florida Current, *Geophys. Res. Lett.*, *40*, 349–353, doi:10.1002/grl.50115.

Haines, K., M. Valdivieso, H. Zuo, and V. Stepanov (2012), Transports and budgets in a 1/4°global ocean reanalysis 1989–2010, *Ocean Sci.*, *8*(3), 333–344.

Haines, K., V. N. Stepanov, M. Valdivieso, and H. Zuo (2013), Atlantic meridional heat transports in two ocean reanalyses evaluated against the RAPID array, *Geophys. Res. Lett.*, *40*, 343-348, doi:10.1029/2012GL054581.

Hall, M. M., M. McCartney, and J. Whitehead (1997), Antarctic bottom water flux in the equatorial western Atlantic, *J. Phys. Oceanogr.*, *27*(9), 1903–1926.

Hirschi, J. J.-M., A. Blaker, B. Sinha, A. Coward, B. de Cuevas, S. Alderson, and G. Madec (2012), Chaotic variability of the meridional overturning circulation on subannual to interannual timescales, *Ocean Sci. Discuss.*, *9*, 3191–3238.

Hunke, E., and W. Lipscomb (2010), *CICE: The Los Alamos Sea Ice Model Documentation and Software Users Manual Version 4.1*, Los Alamos National Laboratory, Los Alamos, N. M.

Ingleby, B., and M. Huddleston (2007), Quality control of ocean temperature and salinity profiles–historical and real-time data, *J. Mar. Syst.*, *65*(1), 158–175.

Johns, W., et al. (2011), Continuous array-based estimates of Atlantic ocean heat transport at 26.5°N, *J. Clim.*, *24*, 2429–2448.

Kanzow, T., et al. (2010), Seasonal variability of the Atlantic meridional overturning circulation at 26.5°N, *J. Clim.*, *23*(21), 5678–5698.

Large, W. G., and S. G. Yeager (2004), *Diurnal to Decadal Global Forcing for Ocean and Sea-Ice Models: The Data Sets and Flux Climatologies*, National Center for Atmospheric Research, Boulder, Colo.

Latif, M., and N. S. Keenlyside (2011), A perspective on decadal climate variability and predictability, *Deep Sea Res. Part II*, *58*(17), 1880–1894.

Madec, G. (2008), *NEMO Ocean Engine*, Institut Pierre-Simon Laplace (IPSL), Paris, France.

Martin, M., A. Hines, and M. Bell (2007), Data assimilation in the FOAM operational short-range ocean forecasting system: A description of the scheme and its impact, *Q. J. R. Meteorolog. Soc.*, *133*(625), 981–995.

Matei, D., H. Pohlmann, J. Jungclaus, W. Müller, H. Haak, and J. Marotzke (2012a), Two tales of initializing decadal climate prediction experiments with the ECHAM5/MPI-OM model, *J. Clim.*, *25*(24), 8502–8523.

Matei, D., J. Baehr, J. H. Jungclaus, H. Haak, W. A. Müller, and J. Marotzke (2012b), Multiyear prediction of monthly mean Atlantic meridional overturning circulation at 26.5°N, *Science*, *335*(6064), 76–79.

McCarthy, G. D., E. Frajka-Williams, W. E. Johns, M. O. Baringer, C. S. Meinen, H. L. Bryden, D. Rayner, A. Duchez, C. Roberts, and S. A. Cunningham (2012), Observed interannual variability of the Atlantic meridional overturning circulation at 26.5°N, *Geophys. Res. Lett.*, *39*, L19609, doi:10.1029/2012GL052933.

McManus, J., R. Francois, J.-M. Gherardi, L. Keigwin, and S. Brown-Leger (2004), Collapse and rapid resumption of Atlantic meridional circulation linked to deglacial climate changes, *Nature*, *428*(6985), 834–837.

Mielke, C., E. Frajka-Williams, and J. Baehr (2013), Observed and simulated variability of the AMOC at 26°N and 41°N, *Geophys. Res. Lett.*, *40*, 1159–1164, doi:10.1002/grl.50233.

Rayner, D., et al. (2011), Monitoring the Atlantic meridional overturning circulation, *Deep Sea Res. Part II*, *58*(17), 1744–1753.

Roberts, C. D., F. Garry, and L. Jackson (2013), A multi-model study of sea surface temperature and sub-surface density fingerprints of the Atlantic meridional overturning circulation, *J. Clim.*, doi:10.1175/JCLI-D-12-00762.1.

Storkey, D., et al. (2010), Forecasting the ocean state using NEMO: The new FOAM system, *J. Oper. Oceanogr.*, *3*(1), 3–15.

Thomas, M., and X. Zhai (2013), Eddy-induced variability of the meridional overturning circulation in a model of the North Atlantic, *Geophys. Res. Lett.*, *40*, 2742–2747, doi:10.1002/grl.50532.

Vellinga, M., and R. Wood (2002), Global climatic impacts of a collapse of the Atlantic thermohaline circulation, *Clim. Change*, *54*(3), 251–267.

Waters, J., D. Lea, D. Martin, M. Storkey, and J. While, (2013), Describing the development of the new FOAM-NEMOVAR system in the global 1/4°configuration, *Forecasting Research Technical Report 578*, Met Office, Exeter, UK.

Yeager, S., A. Karspeck, G. Danabasoglu, J. Tribbia, and H. Teng (2012), A decadal prediction case study: Late twentieth-century North Atlantic ocean heat content, *J. Clim.*, *25*(15), 5173–5189.

Zuo, H., M. Valdivieso, D. Lea, and K. Haines (2013), Global Ocean Physics Reanalysis UR025.4 (1989–2010) as part of the VALue of the RAPID-WATCH Climate Change programme array (VALOR) project, *NCAS British Atmospheric Data Centre*, Available from http://badc.nerc.ac.uk/view/badc.nerc.ac.uk__ATOM__ACTIVITY_cbabde16-df0c-11e2-9e98-00163e251233, doi:10.5285/4bcfa3a4-c7ec-4414-863d-caeceb21f16f.

Erratum

In section 3.3, paragraph [13], the phrase "and the phase of the FC seasonal cycle is inaccurate in ASSIM-3DVAR (Figure 3)" should read "and the phase of the FC seasonal cycle is inaccurate in ASSIM-AC (Figure 3)." Also, a corrected version of Figure 3 is given below.